



HAL
open science

Complementarities of nanoindentation and atomic force microscopy for exploring micromechanical features of ancient flax fibres

Camille Goudenhoft, Sylvie Durand, Célia Caër, Alessia Melelli, Anthony Magueresse, Olivier Arnould, Eric Balnois, Anita Quiles, Darshil U Shah, Johnny Beaugrand, et al.

► To cite this version:

Camille Goudenhoft, Sylvie Durand, Célia Caër, Alessia Melelli, Anthony Magueresse, et al.. Complementarities of nanoindentation and atomic force microscopy for exploring micromechanical features of ancient flax fibres. *Composites Part A: Applied Science and Manufacturing*, 2025, 190, pp.108694. 10.1016/j.compositesa.2024.108694 . hal-04861264

HAL Id: hal-04861264

<https://hal.science/hal-04861264v1>

Submitted on 2 Jan 2025

HAL is a multi-disciplinary open access archive for the deposit and dissemination of scientific research documents, whether they are published or not. The documents may come from teaching and research institutions in France or abroad, or from public or private research centers.

L'archive ouverte pluridisciplinaire **HAL**, est destinée au dépôt et à la diffusion de documents scientifiques de niveau recherche, publiés ou non, émanant des établissements d'enseignement et de recherche français ou étrangers, des laboratoires publics ou privés.



Distributed under a Creative Commons Attribution - NonCommercial - NoDerivatives 4.0 International License



Complementarities of nanoindentation and atomic force microscopy for exploring micromechanical features of ancient flax fibres

Camille Goudenhooff^a, Sylvie Durand^b, Célia Caër^c, Alessia Melelli^d, Anthony Magueresse^a, Olivier Arnould^e, Eric Balnois^f, Anita Quiles^{g,h}, Darshil U. Shahⁱ, Johnny Beaugrand^b, Alain Bourmaud^{a,*}

^a Université de Bretagne Sud, UMR CNRS 6027, IRDL, Lorient, France

^b INRAE, UR1268 France BIA Biopolymères Interactions Assemblages, 44316 Nantes, France

^c ENSTA Bretagne, UMR CNRS 6027, IRDL, Brest, France

^d Synchrotron SOLEIL, DISCO beamline, Gif-sur-Yvette, France

^e LMGC, Université de Montpellier, CNRS, Montpellier, France

^f Laboratoire de Biotechnologie et de Chimie Marines (LBCM), EMR CNRS 6076, Université de Brest, Quimper, France

^g Institut Français d'Archéologie Orientale du Caire, Cairo, Egypt

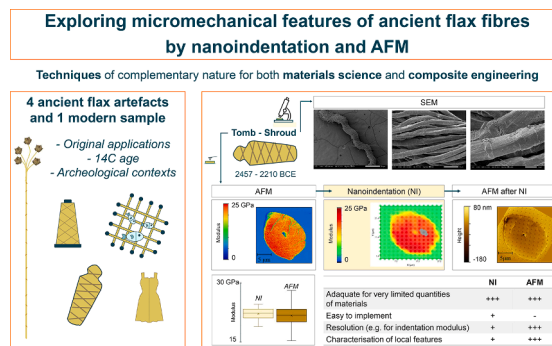
^h Laboratoire de Mesure du Carbone 14 (LMC14), LSCE/IPSL, CEA-CNRS-UVSQ, Université Paris-Saclay, 91191 Gif-sur-Yvette, France

ⁱ Centre for Natural Material Innovation, Department of Architecture, University of Cambridge, Cambridge CB2 1PX, United Kingdom

HIGHLIGHTS

- Four archaeological flax artefacts are examined by coupling nanoindentation and AFM.
- The fine scale approach characterises fibre ultrastructural and mechanical features.
- Nanoindentation is ideal for easily highlighting different degradation phenomena.
- AFM allows a rich study of local heterogeneities in the cell wall of altered fibres.
- This methodology is of interest for materials science and composite engineering.

GRAPHICAL ABSTRACT



ARTICLE INFO

Keywords:

Flax cell wall
SEM
Nanoindentation
AFM
Ageing
Mechanical properties
Ultrastructure

ABSTRACT

The use of flax (*Linum usitatissimum* L.) fibres for textile dates back to several millennia; in Ancient Egypt flax was widely used in many everyday items. While flax fibres continue to diversify today as composite reinforcements, the study of their historical use is highly relevant when it comes to their durability; archaeological samples offer unique lenses for understanding changes in intrinsic fibre properties after long-time periods. Through a comprehensive examination of ancient Egyptian flax fibres from four archaeological artefacts, this study carries out a detailed characterisation of the fibre ultrastructure and micromechanical properties by combining nanoindentation (NI) and atomic force microscopy (AFM). This work highlights the complementary of these techniques for both heritage and materials science; it demonstrates on some samples, the remarkable cell wall

* Corresponding author.

E-mail address: alain.bourmaud@univ-ubs.fr (A. Bourmaud).

<https://doi.org/10.1016/j.compositesa.2024.108694>

Received 26 September 2024; Received in revised form 12 December 2024; Accepted 23 December 2024

Available online 26 December 2024

1359-835X/© 2024 The Authors. Published by Elsevier Ltd. This is an open access article under the CC BY license (<http://creativecommons.org/licenses/by/4.0/>).

stiffness, even after thousands of years, which is a key element for the bio-based composites sector, to better understand the degradation mechanisms of plant fibres.

1. Introduction

The study of ancient plant fibres provides valuable insights on the development of damages within the fibre cell walls over time, in specific contexts and conditions; this knowledge is of interest as such fibres are now being used to design more environmentally friendly engineering materials [1]. Among these, flax-based composites are a prime candidate. Used for thousands of years in the manufacture of textiles, ropes, and even mummy wrappings by the Egyptians [2–6], flax fibres are experiencing a revival of interest in both the textile and materials industries, especially in the automotive, sports and leisure sectors [7]. Consequently, the durability of its performance and intrinsic properties is becoming a major issue, particularly for outdoor applications where the presence of water or microorganisms can lead to rapid and significant ultrastructural degradation [8,9]. Accelerated ageing or composting studies [10] can help understand these degradations, but do not give a complete long-term picture. In this regard, archaeological organic samples represent an incredible resource for exploring the effects of time on plant cell walls in respect with their preservation conditions. They can also provide answers to scientists and industry professionals, as well as future end-users of these fibres, about their sustainable use in the materials sector.

Flax fibres have a multi-layer structure, with a primary cell wall and a secondary cell wall itself composed of several layers: S1, S2 (also called G) and sometimes S3 (also called Gn) [11,12]. The main layer S2 or G layer, is characterised by its high thickness and its great cellulose content, cellulose being in this main layer in the form of microfibrils with a low microfibrillar angle, conferring high mechanical properties to elementary flax fibres [13]. Nevertheless, plant fibres may be sensitive to several factors over ageing that can induce changes in fibre properties [14–16]. The ageing mechanisms of plant fibres are generally attributed to the action of water [17,18] or temperature [15,16] which can have pronounced effects on the structure of cellulose or lignin, and lead to alteration of non-cellulosic polymers. In the case of flax, the lignin fraction is reduced, and matrix polymers such as hemicelluloses and pectins are the most impacted by ageing [6,19]. These damages exhibit significant similarities with fibres aged in compost. These studies have been able to identify three major characteristics in terms of damage: i. microcracks may develop in the plant cell walls [20], ii. alteration of the fibre starts from within (*i.e.* its central lumen) that probably facilitates the circulation of water and micro-organisms [9], and iii. plant fibres have specific damage or defect zones, called kink-bands [21].

It is possible to mechanically characterise samples of yarns or fibres using different experimental methods such as tensile tests [22,23]. Nevertheless, performing tensile tests on ancient elementary fibres or yarns is challenging because such fibres are generally short and brittle, and the experiments are destructive. In addition, tensile tests also require longer samples in (relatively) large quantities, which is a major limitation in the case of precious archaeological samples. More localised mechanical characterisation by nanoindentation (NI) or atomic force microscopy (AFM) is therefore well suited for short plant fibres [24,25] and is also of interest especially as the requisite quantities are much lower (only a few mg). However, they are therefore also less statistically representative than tensile tests (on a much larger number of fibres). Nevertheless, there are only few studies dedicated to the investigation of local mechanical properties of ancient fibre artefacts in literature. Research on the characterisation of ancient flax fibres generally show a relative stability of their indentation modulus [19,20]. In this context, the indentation modulus is used to characterise the cell wall stiffness. This modulus can be obtained by nanoindentation [24–26], as well as by AFM in peak-force quantitative nano-mechanical property mapping (PF-

QNM) mode [27]. Nevertheless, the two techniques have major differences. In nanoindentation, there is a plastic deformation during the loading stage with a residual indentation; the Oliver-Pharr model [28] is used to calculate the indentation modulus from the unloading slope using a pyramidal Berkovich indenter and a low displacement frequency. In the case of the AFM, there is no plastic deformation during the loading stage, without residual indentation; a spherical indenter is used with a high frequency of oscillation, and the indentation modulus is obtained with the Derjagin-Muller-Toporov (DMT) model [29]. Finally, in AFM, the measurement is done in the very first nm of the samples *i.e.* very close to its surface, whereas the nanoindentation depth is generally about 120 nm for wood or plant cell walls [30]. After a fine calibration step in AFM, the two techniques yield similar values.

However, the resulting indentation moduli cannot be simply used to compute the longitudinal modulus of elasticity in tension, using a single “average” Poisson’s ratio. As the cell wall is anisotropic, the value of the indentation modulus is influenced by the transverse, longitudinal, and shear moduli, considering the geometry of the indenters [25,26,31]. In addition, the cellulose microfibrils undergoing compression under the indentation load, microfibril buckling can occur [32,33]. Many works from the wood community highlight that this indentation modulus depends on the characteristics of cellulose [25,26,34]; it is largely influenced by the amount of cellulose present in the walls [26], as well as the microfibrillar angle (MFA) of the cellulose [25,26]. Indeed, its value is directly linked to the response of cellulose microfibrils that undergo buckling during the indentation test [32,33]. Its value and distribution can also be influenced by the direction and angle of cutting during sample preparation [35]. Indentation tests also provide hardness values (the ratio between the maximum applied force and the residual projected contact area estimated from the indentation depth). Unlike the indentation modulus, hardness is more impacted by the amorphous matrix polymers of the cell wall [34], such as pectins and hemicelluloses in flax; indeed, these are responsible for the cohesion of the plant wall [36], and their alteration leads to a decrease in the lateral binding of the cellulose chains and in the local density [25,37], which are considered to be directly related to the plastic behaviour and therefore to the hardness value. This alteration can also lead to a decrease in the cell wall yield stress, impacting hardness [37]. These phenomena have been highlighted by different teams after thermal [38–40] and steam [37] treatments, or by studying plant cell walls with different compositions or levels of growth maturity [41].

In the present work, a number of ancient flax samples, sourced from different museum collections and with very different ageing and conservation histories, were finely characterised by nanoindentation and AFM in mechanical mode. After visualising the samples through scanning electron microscopy (SEM), the work focuses on the nanoindentation measurements and the mechanical differentiation of the samples in relation to their origin and damage. Subsequently, the results of AFM and nanoindentation, performed successively on the same fibres and at the same location, are compared in terms of scale and the respective contributions of the techniques. The relevance of coupling these two technologies for the mechanical analysis of ancient archaeological samples is then discussed.

2. Materials and methods

2.1. Flax samples

2.1.1. General information and labelling

A brief description of the objects studied in this paper is given in Table 1.

More precisely, a batch of modern flax fibres was used as a reference and labelled “modern”. Then, three archaeological flax textiles were selected from the Egyptian collection of Le Louvre Museum (France): E 27370, AF 11258 and E 22924. Finally, one was selected from the Egyptian Museum in Turin (Italy): S. 13268. The selection was based on the knowledge of the archaeological context in which samples were found, the quantity of fabrics and their quality of preservation. All samples were collected under the supervision of the museum curators. For each archaeological object, small pieces of yarn of 10–20 mm were collected for the investigations.

2.1.2. Further information about the flax samples and/or archaeological context

The modern flax sample (“modern”) originates from plants cultivated in 2022 in Normandy (France), mechanically combed and stretched by the French Filature company (Saint-Martin-du-Tilleul, France).

E 27,370 (“mine”) was sampled from the cloth of a small female clay figurine cloths. Radiocarbon dating carried out at the LMC14 lab (Saclay, France) shows that it dates back to the middle of the Second Intermediate period- start of the New Kingdom (1617–1451 calBCE, [42]). This flax textile was found buried in soil, in the galena mines of Gebel el-Zeit. This mining site contained a sanctuary devoted to the Egyptian goddess Hathor, the mistress of galena, used from the Middle Kingdom to the New Kingdom [43]. This object was selected because some contamination is expected due to the constant contact with a desertic soil, regardless of the protection from light as well as humidity and temperature changes provided by its burial within the ground [44].

S. 13,268 (“tomb – shroud”) originates from a tomb of the northern necropolis of Gebelein, from the Old Kingdom time period, and more specifically it consisted in a flax shroud wrapping the mummy of Ini. In his time, Ini was a high priest and the treasurer of the king of lower Egypt [45]. Thus, the shroud in question must have been chosen at the time for its good quality and finesse, due to the high nobility of the deceased. Additionally, this object from a tomb must have been well-protected from light as well as humidity and temperature changes over the millennia before it was discovered by archaeologists.

AF 11,258 (“tomb – unknown”) is an undecorated fragment of fabric from an unknown tomb. Although the archaeological context of this sample remains unknown, it was selected because it visually appears more altered than the other samples (darker colour and holes in certain areas of the fabric).

E 22,924 (“fishing net”) is currently exposed at Le Louvre Museum and consists in an ancient fishing net from the New Kingdom time period. However, its archaeological excavation site is unknown. The dating procedure (carried out at KIK-IRPA, The Royal Institute for Cultural Heritage, Belgium) coupled with FTIR analysis revealed the presence of an exogenous compound (a consolidation treatment applied by

the museum curators), to be eliminated by solvent pretreatment prior to the effective dating.

2.2. SEM observations

A few millimetres of yarn were used and glued on a conductive carbon tape for each selected sample. Prior to examination, a thin coating of gold was deposited on each of the samples using an Edwards Scancoat Six metallization device for 180 s. Then, a JEOL JSM-IT500HR scanning electron microscope was used to analyse the flax samples, based on secondary emission electrons at an accelerating voltage of 3.0 kV.

2.3. Preparation of samples for nano-mechanical investigations

A subsample was cut to a length of < 5 mm for each sample and placed in a flat silicone embedding mould (Polysciences) along the longitudinal direction. These subsamples were embedded in Agar resin (epoxy resin Agar Low Viscosity Resin (LV) – Agar scientific UK) and placed in an oven at 60 °C overnight to cure the resin. Resulting blocks were then machined to reduce their cross-section and height and then glued to a 12 mm AFM stainless steel mounting disk. Each sample surface was trimmed using an ultramicrotome (Ultracut S, Leica Microsystems SAS, France) equipped with diamond knives (Trim and Ultra AFM, Diatome, Switzerland) to remove thin sections (60 nm thick for the final step) at reduced cutting speed (~1 mm/s) for obtaining a “mirror flat surface” required for nanoindentation and AFM measurements.

For the sake of comparison of the nano-mechanical investigations, the same fibres and more specifically the same cross-section regions were studied by both AFM and NI, starting the experiments with AFM PF-QNM (see Fig. 1). However, the investigations are described here by first presenting the NI to structure the study. In addition, nano-mechanical investigations were performed in a climate-controlled room (air conditioning), namely 23 °C and 50 % RH.

2.4. Nanoindentation

Nanoindentation measurements were conducted with a TI 980 Triboindenter device (Bruker Hysitron), fitted with a numerical microscope and a NanoDMA III transducer equipped with a Berkovich-shaped diamond tip. Prior to nanoindentation experiments, calibration steps were all successfully performed (*i.e.* indentation axis, optic-probe tip offset, machine compliance and probe tip area function). The study is conducted on carefully selected fibres with a suitable orientation, *i.e.* allegedly perpendicular to the cutting plane. The nanoindentation tests were finally performed following a protocol described in a previous study [46], namely using the Bruker’s Hysitron XPM Accelerated Property Mapping mode (XPM Hysitron, Bruker), with an indentation

Table 1

A brief description of the different artefacts studied in the present work and the respective used labelling.

Object / Inventory number	Labelling used in the present work	Lab code	14C Age (BP)	Calibrated range (calBCE)	Archaeological context
Modern sample	Modern	N/A	N/A	N/A	Combed and stretched flax fibres, cultivated in 2022 in Normandy (France), mix of several textile varieties
E 27,370	Mine	SacA 19,498	3259 ± 34 BP	1617 – 1451calBCE (94.5 %) [IntCal13]	Textile used as a dress for female clay figurine found buried in the sanctuary of Gebel el-Zeit (galena mines)
S. 13,268	Tomb – Shroud	SacA 59,904 SacA 59,905 SacA 59,906	3865 ± 30 BP 3845 ± 30 BP 3875 ± 30 BP	2457 – 2210calBCE (95.4 %) [IntCal20] combined density	Flax fabric from the outer shroud found in the tomb of Ini
AF 11,258	Tomb – Unknown	N/A	N/A	N/A	Textile from an unknown tomb
E 22,924	Fishing net	RICH-34,380.2.1	3011 ± 27 BP	1390 – 1120 calBCE (73.1 %) [IntCal20]	Fishing net from an unknown archaeological site

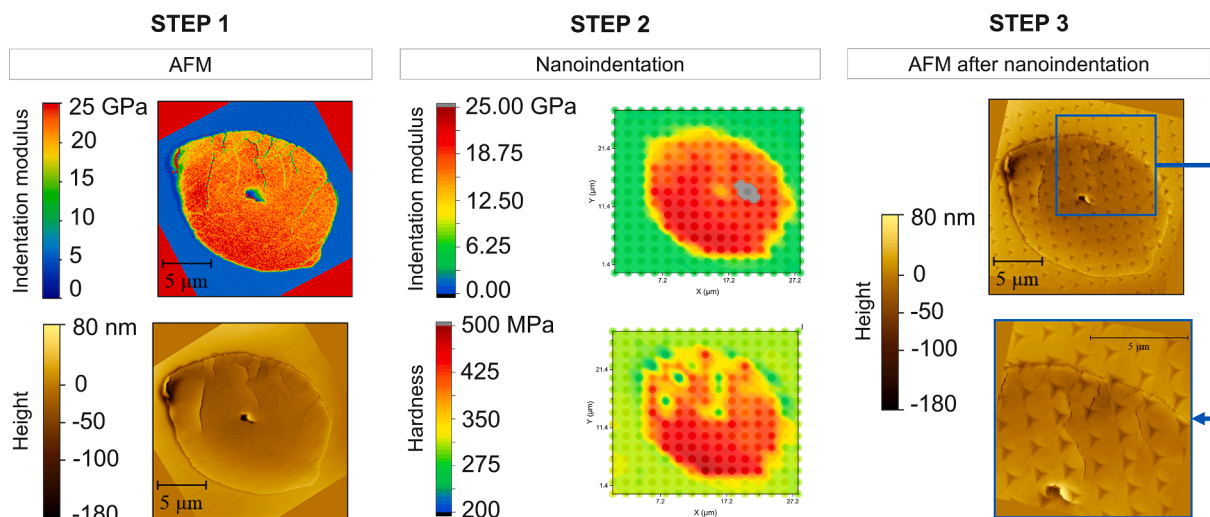


Fig. 1. Presentation of the different steps performed for the analysis of the same fibre (or neighbouring fibres). STEP 1: AFM in mechanical mode is first performed (to avoid subsequent AFM mapping of the indent matrices generated by NI, which would greatly complicate nanomechanical measurements of the fibre cell walls using AFM); the indentation modulus as well as fibre morphology and local defects are evaluated. STEP 2: Nanoindentation is performed; indentation modulus and hardness are estimated. STEP 3: when relevant, an AFM analysis of the topography is performed after nanoindentation to evaluate the effect of indentation on the aspects of local defects.

cycle of 0.1 s loading – 0.1 s holding at maximum load controlled of 180 μN – 0.1 s unloading, a data acquisition rate of 1000 pts/s and a lateral move speed of 10 μm/s, approximately centred on the fibre of interest (previously studied by AFM). The mapping consisted in an array of 15 x 15 (or more rarely 22 x 22 for a larger area of interest), with a spacing of 2 μm between indents. Thanks to this procedure, both indentation modulus and hardness were calculated through equations given by Oliver and Pharr [28], using the slope of the unloading curve. Finally, the values obtained using XPM mapping are sorted to retain only those thought to be associated with indentations that occur only in the fibre cell wall (see Supplementary figure 1).

2.5. AFM investigations

A Multimode 8 Atomic Force Microscope (Bruker, Billerica, Massachusetts, USA) was operated using the PF-QNM mode, and equipped with a RTESPA-525 probe (Bruker probes, Billerica, Massachusetts USA) with a resonance frequency around 525 kHz and a nominal spring constant around 200 N/m. With each probe, the actual spring constant was assessed with the Sader Method (<https://sadermethod.org/>), and the AFM set-up calibrated with the relative method using sapphire to calculate the deflection sensitivity and the PF-QNM synchronization distance. A sample of aramid fibres K305 Kevlar Taffetas 305 g/m² (Sicommin epoxy systems, France) prepared with the same protocol as described previously (2.3. Preparation of samples for nano-mechanical investigations) was used to calibrate the tip radius. The fast scan axis angle was set at 90°, the maximum peak force setpoint was 200 nN, the oscillation frequency set at 2 kHz. The scan frequency was selected at 0.150 Hz maximum, and the image resolution set to 256 x 256 pixels. The recorded force-distance curves obtained were automatically adjusted using Nanoscope Analysis software (Bruker, Palaiseau, France) and the indentation modulus is obtained based on the Derjaguin-Muller-Toporov (DMT) contact model [29] adjusted on the unloading part of the curve. As flax fibre cell wall is anisotropic, it makes no sense to calculate Young's modulus from the indentation modulus and a Poisson's ratio [26], so the “raw” value of the indentation modulus is kept. In this aim, the Poisson's ratio is set at 0 in the software for all samples so that the elastic modulus map given is that of the indentation modulus, to be compared then to the one obtained by NI [28,47,48]. Moreover, in order to analyse the values of the indentation modulus obtained by AFM of the cell wall of a flax fibre only, the surface of the considered wall was

selected from each AFM image and the statistical pre-treatment of this area (mean value, standard deviation) was obtained using Gwyddion free software (see Supplementary figure 2).

2.6. Statistical analysis

To evaluate the statistical difference in terms of mean values of fibre mechanical performances, the results of nanoindentation tests were analysed using a bilateral *t*-test with a 95 % confidence interval. For a given sample, both the indentation modulus and the hardness values are analysed one by one against the corresponding results of the other samples; each sample was therefore statistically compared to each other based on two fibre properties (indentation modulus and hardness). If the *P*-value resulting from the *t*-test is greater than 0.05 ($P > 0.05$), the difference in the fibre property is not statistically significant. Thus, when two mechanical characteristics per sample are used for comparison, samples will be considered to have similar mechanical properties if both their indentation modulus and hardness are not statistically different ($P > 0.05$). Conversely, samples will be considered different in terms of mechanical properties if at least a pair of such properties, indentation modulus and/or hardness, are considered to be statistically different ($P < 0.05$).

3. Results and discussion

3.1. Investigation of the specificities of each archaeological sample through SEM analysis

SEM micrographs in Fig. 2 show the overall aspects of modern and archaeological fibres from the various samples of interest for the present study.

At this observation scale, fibres from the “modern” batch (in green) appear as bundles but well individualised due to the successive combing and stretching processes, the surface of the fibres seems rather homogeneous and smooth, and some minor defects (also called “kink-bands”, marked with yellow arrows on the SEM images) can be observed. On the other hand, the fibres from the “mine” sample (in red) are also well individualised but have a very degraded, textured/rough appearance, where the cellulose microfibrils can be seen, suggesting that the outermost layers, *i.e.* primary cell wall and also S1, have disappeared somehow. In addition, small particles or agglomerates attached to some

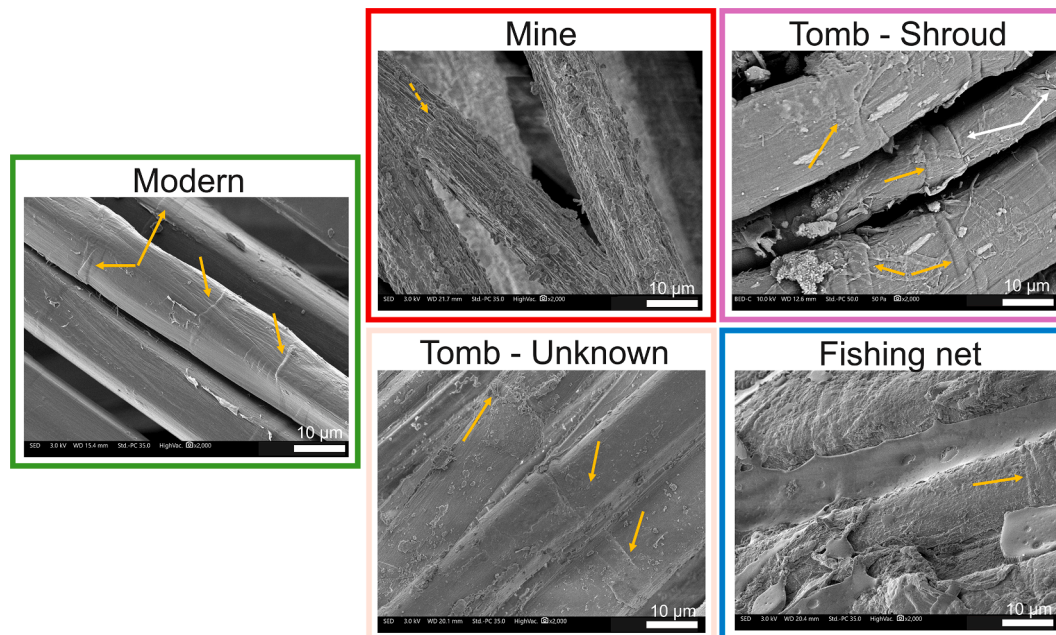


Fig. 2. SEM images of modern and ancient flax fibres from archaeological textiles of interest (same scale). The yellow arrows point to kink-bands, the white ones to crack-like defects. (For interpretation of the references to colour in this figure legend, the reader is referred to the web version of this article.)

macrofibrils can be spotted. The fibres of the “tomb – shroud” sample (in pink) seem quite individualised and show several kink-bands; one can also see the appearance of crack-like defects (white arrows). Some contamination is laid on the surface. The “tomb – unknown” sample (in beige) has kept a good cohesion between the fibres, visible as bundles of fibres, linked together by a cohesive substance, more homogenous than middle lamellae, being possibly a residue of coating or treatment. Few kink-bands are present, and some small particles on the surface of the fibres help to distinguish this sample, which despite its age, has a very similar appearance to the “modern” one. Finally, the sample “fishing net” (in blue) has a coating for consolidation visible between the fibres, glueing the fibres together. In areas where fibres are visible, the surface shows irregularities similar to a roughening, possibly consisting in a crust-like deposited extra-layer. A kink-band can be seen on one of the fibres. The original purpose of this coating made of organic matter is most probably to protect the fibres from further degradation and for a better handling of the archaeological object in the museum, while the authors assume that the crust-like layer including Si, Fe and Al (highlighted through SEM-EDX analysis, data not shown) was formed over millennia prior to intervention of the curators and is now visible only in areas where the consolidation matrix is missing. These main features are summarised in Table 2. As a result, these SEM images can be used to highlight various ageing features such as different fibre organisations within the yarns, fibres having interesting morphological characteristics, as well as features of local defects, being very specific for each sample. However, most of these specificities cannot be directly explained by the age of the samples, but rather by the preservation conditions and/or the original use of the textile material.

3.2. Analysis of the fibre nano-mechanical features through NI measurements

Nanoindentation experiments were conducted to evaluate the indentation modulus M and hardness H across several fibres per sample of interest. Fig. 3 shows the hardness values obtained as a function of the indentation modulus values for each of the indents made in the different fibres. To make Fig. 3 easier to read and interpret, clusters are schematised. Complementary to Fig. 3, Table 3 summarises the average and standard deviation of the modulus and hardness values

Table 2

Main features of the different samples highlighted by SEM analysis.

Label used in the present work	Main features highlighted by SEM
Modern	Fibres in the form of well individualised bundles Homogeneous and smooth surface Some slight kink-bands
Mine	Well individualised fibres Very degraded appearance (the outermost layers are gone, making inner cellulose macrofibrils visible) Small agglomerates attached to microfibrils
Tomb – Shroud	Intermediate level of individualisation Dispersed contamination on the surface Some kink-bands Additional defects like cracks without preferential orientation
Tomb – Unknown	Fibres tightly attached as bundle with the presence of a “glue” between fibres Relatively homogeneous surface with some particles Presence of kink-bands
Fishing net	Fibres hardly visible but glued together through an extra-coating for consolidation Presence of a heterogeneous crust-like layer on the fibre surface in absence of coating

obtained for each of the samples of interest.

One can notice from the clusters shown in Fig. 3 that each sample exhibit different average mechanical properties compared to the other samples in the study. This is complemented with the statistical analysis (t -test), whose results are symbolised by the superscript letters in Table 3), highlighting that only the indentation modulus of “modern” and “mine” are not statistically different, while only the hardness of “modern” and “tomb – unknown” are not statistically different. Thus, none of the samples have both an indentation modulus M and a hardness H that can be considered statistically similar with another sample.

When considering the indentation modulus, the samples “modern” and “mine” exhibit the highest average values, even considered to be

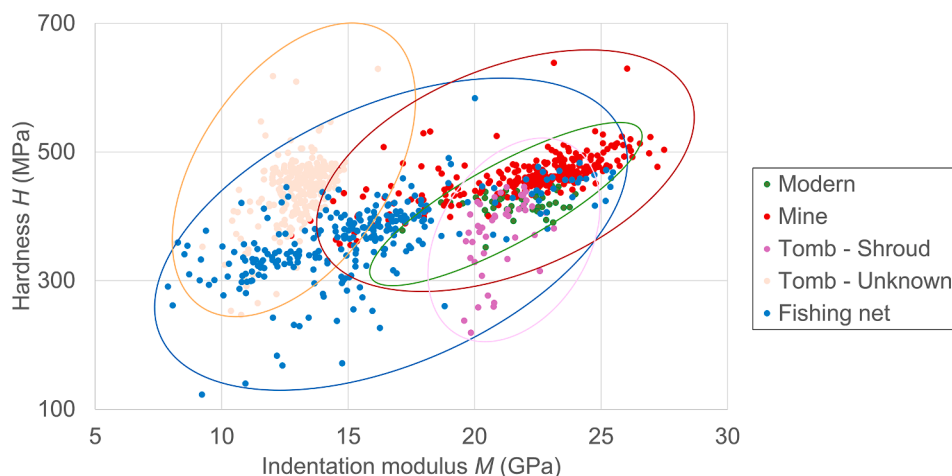


Fig. 3. Hardness H as a function of indentation modulus M obtained by nanoindentation on several fibres from modern and ancient samples.

Table 3

Average and standard deviation of the mechanical properties of modern and ancient fibres obtained by nanoindentation. The superscript letters specify that the results of statistical t-tests, and similar superscript letters indicate that the mean values are not statistically different ($P > 0.05$).

Sample	Number of fibres	Number of indents	Average indentation depth (nm)	Indentation modulus M (GPa)	Hardness H (MPa)	H/M (%)
Modern	3	227	123 ± 5	22.0 ± 2.0 ^a	441 ± 29 ^e	2.0 ± 0.2
Mine	6	274	120 ± 6	22.1 ± 2.9 ^a	462 ± 35 ^f	2.1 ± 0.2
Tomb – Shroud	2	130	132 ± 12	19.3 ± 1.9 ^b	399 ± 58 ^g	2.1 ± 0.2
Tomb – Unknown	3	279	129 ± 9	13.0 ± 1.0 ^c	442 ± 49 ^e	3.4 ± 0.4
Fishing net	4	266	141 ± 16	15.5 ± 3.9 ^d	366 ± 62 ^h	2.4 ± 0.5

statistically similar, despite a slightly higher standard deviation for the ancient sample, and in spite of the very degraded aspect of these ancient fibres illustrated through scanning electron microscopy (SEM) (see Fig. 2 and Table 2). This assessment is in line with previous findings on the “mine” sample from Melelli et al. [6]; using SHG multi-photon and deep UV microscopy, it was demonstrated that the biochemical composition of the “mine” sample was relatively well preserved compared to other historical artefacts. The sample “tomb – shroud” exhibits a high modulus as well, despite defects on the fibres from the SEM images. The fibres from “tomb – unknown” have the lowest modulus, although they look very similar to modern fibres, with very little dispersion. Finally, the sample “fishing net” exhibits an intermediate average indentation modulus but the greatest dispersion of fibre properties highlighted by NI; this dispersion is evidence of a non-homogenous – and sometimes advanced – degradation of flax fibres in the “fishing net”, explaining the need to apply a consolidation agent to this archaeological object (visible in the related SEM image in Fig. 2). Previous investigations have also demonstrated the high degradation level of some fibres in the “fishing net” samples: some fibres exhibit important structural and biochemical changes through multi-photon and deep-UV microscopy, with the degradation of non-cellulosic components and even a pronounced degradation of the cellulose part [6].

When focusing on the hardness values, the sample “mine” shows the highest average hardness, followed closely by “tomb – unknown” and “modern” with statistically similar values. The sample “tomb – shroud” exhibits an average hardness of about 90 % of the “modern” value. Finally, the sample “fishing net” displays the lowest average hardness with the greatest dispersion, that could also be attributed to the sample advanced and heterogeneous ageing suggesting a degradation of non-cellulosic polymers (NCPs) along time [34].

Thus, in the present study, it is difficult to make the link between the aspects of the fibres and the nano-mechanical properties obtained in nanoindentation. A visually very marked degradation of fibres on SEM

images (e.g. for the “mine” sample) does not imply a drop in mechanical performance at the cell wall scale; conversely, a well-preserved aspect of the fibres (e.g. with the “tomb – unknown” sample) does not imply high local mechanical properties at the cell wall scale.

In addition, interestingly, “tomb – unknown” shows the lowest indentation modulus but a high average hardness compared to the other samples. This is well-illustrated by the ratio H/M given in Table 2, being higher for this sample, while the other samples – including the “modern” one – have ratios of the same order of magnitude, highlighting a similar trend between hardness and indentation modulus evolution. As mentioned in the introduction, in literature, the indentation modulus is generally associated with the cellulose whereas hardness values are with non-cellulosic polymers [25,34]. In this case, for all the archaeological samples except for “tomb – unknown”, it is not possible to say that ageing has preferentially degraded NCPs or cellulose from the nano-indentation data, the H/M ratio remaining like that of the “modern” reference flax. On the other hand, the increase in H/M for “tomb – unknown” would suggest a preferential degradation of cellulose (due to the drop in the average value of M as well as the increase in the H/M ratio). This is a debatable hypothesis given the preserved appearance of the fibres in SEM and the fact than NCPs usually demonstrate a greater sensitivity to ageing than cellulosic parts [20]. Nevertheless, this sample was conserved in a tomb with possibly low temperature, humidity and UV variations, in favour of a relative stability of NCPs properties. Regarding the decrease in indentation modulus, it can be induced by a decrease of cellulose properties, including structural parameters or crystallinity degree but also by buckling of cellulose macrofibrils.

To investigate further the relationship between the specific general features (including ageing conditions, original uses, aspect of the fibres) of the samples and the fibre mechanical properties characterised by nanoindentation, a special interest is given to 1 (or 2 neighbouring) fibre (s) for each batch. For this more restricted analysis, fibres with properties close to the average values are carefully selected, and resulting

XPM mappings of the indentation modulus M and hardness H are given in Fig. 4A.

These mappings highlight the presence of a lumen at the centre of the fibres (and excluded from calculations of the mechanical properties of the fibres as presented in Supplementary figure 1), commonly present in flax fibres. Heterogeneities (visible for both M and H) can also be seen in the mapping. For more details, it is preferable to study the associated box-and-whisker boxes (Fig. 4B and C).

In terms of indentation modulus (Fig. 4B), the values obtained for ancient fibres seem to be more dispersed than for the “modern” one, except for “tomb – unknown”, which has a narrower dispersion in terms of absolute values, indicating a homogenous degradation of stiffness, and consequently of cellulose performance or organisation.

Hardness (Fig. 4C) gives even more contrasting results between the contemporary and archaeological samples. The “modern” sample shows a low dispersion in hardness, the “mine” sample shows a slightly greater dispersion, while the other ancient samples show much widely dispersed values. Though “tomb – unknown” showed little dispersion for M , H values are quite heterogeneous. On the other hand, the hardness mapping of “tomb – shroud” highlights zones of low hardness within the cell wall, which is well-translated by a strong disparity of the hardness value within the box-and-whisker box of the related fibre.

Since a better measurement accuracy is limited by the constraints of the nanoindentation technique itself (indentation depth of more than a hundred nm and the need to space the indents of a few μm to avoid an overlap phenomenon in particular), AFM tests are needed to extend further the study at the cell wall scale and benefit from higher resolute information.

3.3. Analysis of fibre nano-mechanical features through AFM measurements

To enhance the mechanical study at the scale of the fibre cell wall and to investigate further the characteristics of local defects, the AFM technique is deployed on the very same fibres of interest, previously

selected for the nanoindentation discussion. Fig. 5 provides and compares the mappings and average values obtained by both techniques for each considered fibre.

First of all, the AFM results reveal additional information to NI mapping in terms of fibre morphology and defects (Fig. 5A), in line with the observations made by SEM. In fact, the irregular edges of the fibre are highlighted on the AFM image for the sample “mine” and correspond to the macrofibrils visible in SEM as the external layer of such fibres, drawing attention to the advanced degradation of the outer part of the fibre; cracks visible in SEM at the fibre surface of the sample “tomb – shroud” (see Fig. 2 and Table 2) are also visible in the transverse cross-section through AFM analysis and can be related to the zone of lower hardness highlighted previously by nanoindentation (Fig. 3); “tomb – unknown” show some cohesive fibres, with the presence of a thin extra layer (in light blue in the AFM map) similar to a glue (explaining the experimental difficulty to find and map individualized fibres for this batch), this latter layer being also visible on the SEM images; “fishing net” also exhibit two tight fibres, for which edges appear to be quite irregular, in agreement with the SEM images showing a crust-like layer at the fibre surface in the areas without coating.

In addition, the AFM images confirm that there has been no deterioration, either morphological or mechanical, from the lumen, for which the shape and size remains comparable to “modern” for all the archaeological samples. This confirms that the samples were probably kept away from water, as ageing in a humid environment could lead to microbial contamination via the lumen, with a tunnel effect inducing structural damage from the central cavity [9]. Long storage in tombs or arid soil of Egypt prevented this type of degradation. In the case of “fishing net” fibres, the immersion times, probably followed by drying cycles and UV degradation, could cause the heterogeneous degradation within yarn and the creation of the crust-like layer on the fibre surface; however, the influence of the preservation conditions of this artefact (whose archaeological context is unknown) on ageing could also have impacted the ageing homogeneity of flax and the crust generation.

At last, the indentation modulus calculated from NI and AFM are

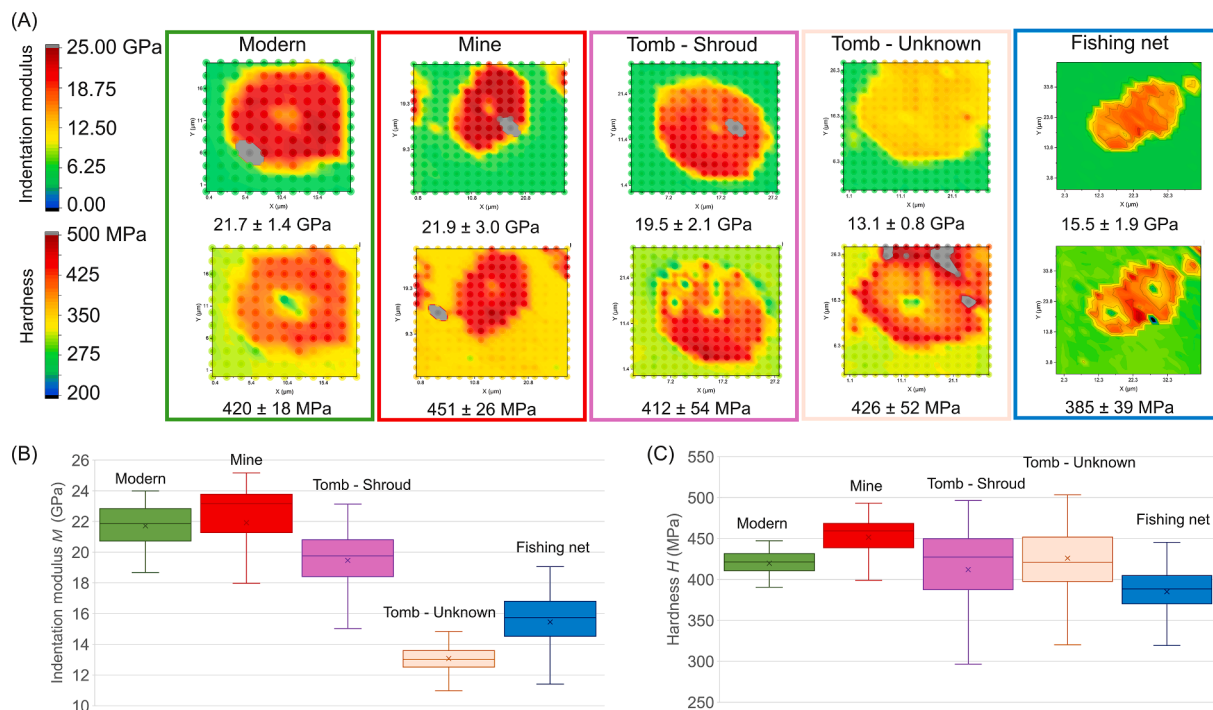


Fig. 4. (A) XPM mapping (indentation modulus and hardness respectively) of modern and archaeological fibres. Grey values represent either outlier values (not taken into account for the analysis) or acceptable value above the high end of the XPM mapping scale (25 GPa for M and 500 MPa for H respectively). (B-C) Associated box-and-whisker boxes of mechanical data ((B) indentation modulus and (C) hardness respectively) are given to illustrate the average properties and dispersion.

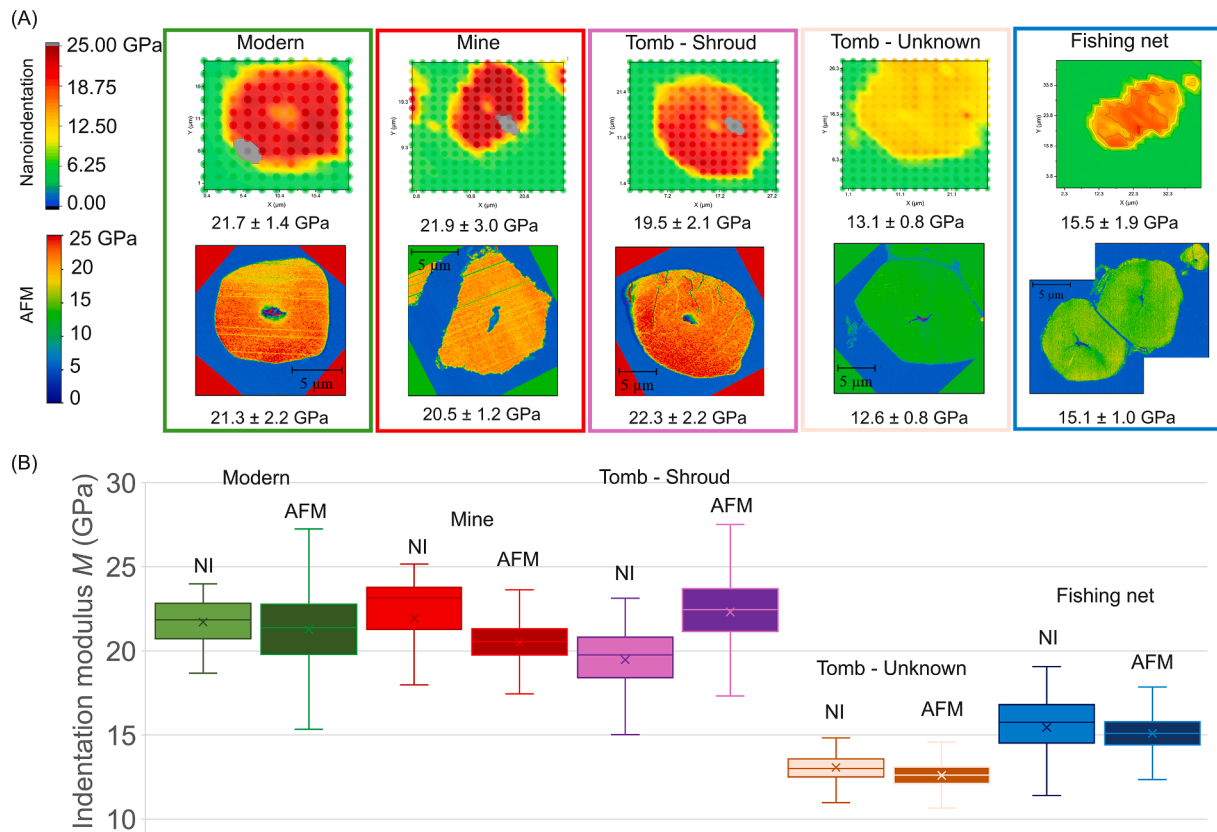


Fig. 5. (A) Comparison of indentation modulus mapping and average values obtained by nanoindentation (top) and AFM (bottom). To facilitate the comparison, AFM images were oriented to best match the position of the fibres on the nanoindentation mappings. In addition, some scratches are sometimes visible on AFM images – fine lines parallel to each other for instance for the sample “mine” – due to the ultramicrotome cut. (B) Associated box-and-whisker boxes, given for each sample and characterisation technique.

relatively homogeneous within the cell wall of a single fibre, whatever the ageing conditions, average performances and heterogeneity of the sample.

For more details on the mechanical data resulting from the two techniques for the fibres under consideration, the associated box-and-whisker boxes are compared in Fig. 5B, and further information on these results are given in Table 4. Hence, despite the different scales of measurement between techniques (size and depth of indentation, number of measurements per fibre, and so on) and the complexity of calibrating the tips for mechanical measurements using AFM PF-QNM, the average moduli obtained with NI and AFM are very comparable. Supplementary figure 3 also highlights that, in case of a sample with lots of heterogeneities between fibres such as the sample “fishing net”, both

Table 4

Complementary information about the values obtained using NI and AFM on the same fibre.

Sample	Number of indents in the cell wall		Hardness H (MPa)		Indentation modulus M (GPa)	
	NI	AFM	NI	AFM	NI	AFM
Modern	46	29,259	420 ± 18		21.7 ± 1.4	21.3 ± 2.2
Mine	50	17,511	451 ± 26		21.9 ± 3.0	20.5 ± 1.2
Tomb – Shroud	85	23,628	412 ± 54		19.5 ± 2.1	22.3 ± 2.2
Tomb – Unknown	88	26,497	426 ± 52		13.1 ± 0.8	12.6 ± 0.8
Fishing net	104	47,976	385 ± 39		15.5 ± 1.9	15.1 ± 1.0

techniques can evidence such features. Moreover, the difference between the values measured by the two techniques is greater for a widespread degradation (“mine”) or when local defects are revealed using AFM (“tomb – shroud”). It may be presumed that the greater dispersion observed with NI on the sample “mine” could be due to the specific nature of the widespread degradation although the nano-indentation technique itself does not allow to illustrate it directly. For such cases, an additional analysis using AFM would be required for more precise local mechanical and/or morphological information, for instance in the case of very localised defects such as cracks. These observations and differences in calculated indentation moduli underline the strong interest of supplementing NI by the high-resolution AFM experiments; thanks to AFM, new pieces of information are provided, accessible through the higher resolution. For example, regarding the “tomb – shroud” sample, the indentation modulus from NI reveals some very low values, while AFM demonstrates that they are probably induced by cracks and that, in the undamaged areas, the indentation modulus is quite stable and homogenous.

3.4. Analysis of fibre features after nanoindentation through AFM measurements

For this last study, the “tomb – shroud” sample was selected, especially for the differences in stiffness observed through NI and AFM. In order to determine whether the discrepancy between the average indentation modulus obtained by AFM and by NI on the “tomb – shroud” sample can be explained by some limitations of the NI technique or by a local modification of the sample in the surrounding of cracks due to NI, an additional analysis step is carried out (see Fig. 1. STEP 3). Thus, the morphological analysis of the topology of samples through AFM was

done before and after NI testing. An example of the images obtained for two distinct fibres of this sample is given in [Supplementary figure 4](#). This close observation by AFM highlights the indents matrices and shows the size of the indentation prints left by the indenter within the fibre cell walls. There does not seem to be any link between the shape or depth of the residual prints and their location (defect-free zone, close to a crack or on a crack), despite differences in hardness highlighted by nanoindentation on XPM mappings. Furthermore, when an indent has been generated on a crack, the latter neither enlarged nor propagated further with nanoindentation. Thus, if there is a difference in the indentation modulus measured using AFM and NI, it is essentially due to the scale (depth and width of the volume probed) and precision of the technique, with AFM revealing local defects that are more difficult to detect using NI and being very sensitive to surface properties over a few nm. For this sample low-scale degradation is certainly occurring, as shown in a previous analysis with second harmonic generation microscopy (SHG) [6], where a poorly intense SHG signal was observed; this phenomenon is possibly due to local disordering of crystalline cellulose, which is a plausible explanation for the mechanical variations observed at the AFM and NI scales. Nevertheless, [Supplementary figure 4](#) emphasizes that defects affect the average mechanical values estimated by NI, and such local defects are highlighted more clearly through measurements of hardness. Therefore, this work demonstrates the complementary nature of both techniques for characterising the specific features of ancient fibres: from the micro-scale of the fibre to the nanoscale of local defects, from the general appearance of fibres and their average mechanical properties to the fine characterisation of local specificities.

4. Conclusion

This work combines complementary characterisation techniques, namely SEM, nanoindentation and AFM, to analyse four samples of ancient flax from various archaeological objects of interest. This combination of techniques enables the investigation at very fine scales, in terms of ultrastructural features and mechanical properties, of precious materials (available in very limited quantities) and fibres that are sometimes very altered. The findings reveal a wide range of local mechanical properties, depending on the initial function of the textiles, but also on their ageing conditions. Some flax cell walls have mechanical properties similar to modern ones, demonstrating the potential durability of flax if the fibres are preserved. Each non/micro-destructive technique is applied the same fibre samples and location to get a consistent and comprehensive picture.

In terms of mechanical features, nanoindentation enables indentation modulus and hardness characteristics to be rapidly assessed on a batch scale from several individual fibres. For instance, “tomb – unknown” shows homogeneous features with a lower indentation modulus than all other samples, while its average hardness remains similar to that the “modern” reference sample. This technique can also be used to quickly underline significant heterogeneity of mechanical features within a single sample (e.g. “fishing net”). For a given elementary fibre, nanoindentation through hardness values can reveal some local heterogeneities within the cell wall but does not allow to conclude on their nature (e.g. “tomb – shroud”).

Finally, for fine-scale analysis of fibre characteristics or to highlight ultrastructural properties linked to local features, *i.e.* from fibre shape, presence of an extra-layer of matrix, lumen size, nature and/or dimensions of local defects such as porosities or cracks, to local indentation modulus with a greater resolution, AFM is a technique of great potential for the precise analysis of altered materials, in this case for the analysis of ancient flax fibres.

In order to facilitate the choice of a particular nanomechanical approach, [Table 5](#) provides a comparative summary of NI and AFM based on a selection of different parameters of interest for the study of plant fibres that may be altered.

Subsequently, it would be interesting to pursue this work in order to

Table 5

Complementary information about the values obtained using NI and AFM on the same fibre.

	Nanoindentation	AFM
Requirements for sample preparation (<i>sample size constraints, quality of surface preparation, etc.</i>)	Demanding	Very demanding
Steps for calibration/data acquisition	Demanding/Rapid	Very demanding/Time-consuming
Mechanical data that can be evaluated	Hardness Indentation modulus	Indentation modulus
Accuracy of average values (<i>reliability/resolution</i>)	Quantitative/Fine-scale	Semi-quantitative/Very fine-scale
Suitable for the study of local heterogeneity	Detection	Precise characterisation

analyse differences in local mechanical behaviour of flax fibres, with a particular focus on the characteristics of residual indents. This focus would be of interest between samples with different degradation conditions, but also at the scale of the walls of a given fibre, to better understand the parallel between a material's durability and the preservation of these local mechanical characteristics. On the other hand, this microstructural approach could be used to locally characterise the reinforcement properties of plant fibre-based composites after artificial ageing or at the end of their industrial life cycle, for instance before recycling these materials.

CRediT authorship contribution statement

Camille Goudenhoft: Writing – original draft, Validation, Methodology, Investigation, Formal analysis, Data curation, Conceptualization. **Sylvie Durand:** Writing – review & editing, Methodology, Investigation, Data curation. **Célia Caër:** Writing – review & editing, Methodology, Investigation, Data curation. **Alessia Melelli:** Writing – review & editing, Methodology, Investigation. **Anthony Magueresse:** Writing – review & editing, Methodology, Investigation. **Olivier Arnould:** Writing – review & editing, Validation, Methodology. **Eric Balnois:** Writing – review & editing, Methodology, Investigation. **Anita Quiles:** Writing – review & editing, Supervision, Conceptualization. **Darshil U. Shah:** Writing – review & editing, Supervision, Conceptualization. **Johnny Beaugrand:** Writing – review & editing, Supervision, Conceptualization. **Alain Bourmaud:** Writing – review & editing, Validation, Supervision, Methodology, Funding acquisition, Formal analysis, Conceptualization.

Declaration of competing interest

The authors declare that they have no known competing financial interests or personal relationships that could have appeared to influence the work reported in this paper.

Acknowledgements

The authors gratefully thank the ANR (Agence Nationale de la Recherche) for funding the ANUBIS project (ANR-21-CE43-0010-ANUBIS). The authors would like to express their gratitude to Roberta Cortopassi (Musée du Louvre, Paris, France), as well as Matilde Borla and Valentina Turina (Museo Egizio, Turin, Italy) for the sampling sessions and sharing their associated historical knowledge. Michel Ramonda (CTM, University of Montpellier, Montpellier, France) is thanked for sharing his technical experience on AFM PF-QNM investigations and improving the related method. IRDL and ENSTA Bretagne gratefully acknowledge “Contrat de Plan Etat - Région Bretagne (CPER)” as well as the “Fonds Européen de Développement Régional (FEDER)” for their financial support to the reported work.

Appendix A. Supplementary material

Supplementary data to this article can be found online at <https://doi.org/10.1016/j.compositesa.2024.108694>.

Data availability

Data will be made available on request.

References

- Mohanty AK, Vivekanandhan S, Pin J-M, Misra M. Composites from renewable and sustainable resources: challenges and innovations. *Science* 1979;2018(362): 536–42. <https://doi.org/10.1126/science.aat9072>.
- Pomey P, Poveda P. Gyptis: sailing replica of a 6th-century-BC Archaic Greek Sewn Boat. *Int J Naut Archaeol* 2018;47:45–56. <https://doi.org/10.1111/1095-9270.12294>.
- Wild FC, Wild JP. Sails from the Roman port at Berenike, Egypt. *Int J Naut Archaeol* 2001;30:211–20. <https://doi.org/10.1006/ijna.2001.0354>.
- Blue L. Myos Hormos/Quşeir al-Qadim. A Roman and Islamic port on the Red Sea coast of Egypt-A maritime perspective. *Proceedings of the Seminar for Arabian Studies* 2002 32 139–50.
- Whitewright J. Roman rigging material from the red sea port of Myos Hormos. *Int J Naut Archaeol* 2007;36:282–92. <https://doi.org/10.1111/j.1095-9270.2007.00150.x>.
- Melelli A, Goudenhooff C, Durand S, Quiles A, Cortopassi R, Morgillo L, et al. Revealing degradation mechanisms of archaeological flax textiles through the evolution of fibres' parietal polymers by synchrotron deep-UV fluorescence. *Polym Degrad Stab* 2024;226:110826. <https://doi.org/10.1016/j.polyimdegradstab.2024.110826>.
- Khalfallah M, Abbès B, Abbès F, Guo YQ, Marcel V, Duval A, et al. Innovative flax tapes reinforced Acrodur biocomposites: a new alternative for automotive applications. *Mater Des* 2014;64:116–26. <https://doi.org/10.1016/j.matdes.2014.07.029>.
- Pantaloni D, Melelli A, Shah DU, Baley C, Bourmaud A. Influence of water ageing on the mechanical properties of flax/PLA non-woven composites. *Polym Degrad Stab* 2022;200:109957. <https://doi.org/10.1016/j.polyimdegradstab.2022.109957>.
- Melelli A, Pantaloni D, Balnois E, Arnould O, Jamme F, Baley C, et al. Investigations by AFM of ageing mechanisms in PLA-Flax fibre composites during garden composting. *Polymers (Basel)* 2021;13:2225. <https://doi.org/10.3390/polym13142225>.
- Pantaloni D, Shah D, Baley C, Bourmaud A. Monitoring of mechanical performances of flax non-woven biocomposites during a home compost degradation. *Polym Degrad Stab* 2020;177:109166. <https://doi.org/10.1016/j.polyimdegradstab.2020.109166>.
- Goudenhooff C, Bourmaud A, Baley C. Flax (*Linum usitatissimum* L.) Fibers for Composite Reinforcement: Exploring the Link Between Plant Growth, Cell Walls Development, and Fiber Properties. *Front Plant Sci* 2019;10:411. doi: 10.3389/fpls.2019.00411.
- Rihouey C, Paynel F, Gorshkova T, Morvan C. Flax fibers: assessing the non-cellulosic polysaccharides and an approach to supramolecular design of the cell wall. *Cellul* 2017;24:1985–2001. <https://doi.org/10.1007/s10570-017-1246-5>.
- Melelli A, Jamme F, Legland D, Beauprand J, Bourmaud A. Microfibril angle of elementary flax fibres investigated with polarised second harmonic generation microscopy. *Ind Crop Prod* 2020;156:112847. <https://doi.org/10.1016/j.indcrop.2020.112847>.
- Garat W, Le Moigne N, Corn S, Beauprand J, Bergeret A. Swelling of natural fibre bundles under hygro- and hydrothermal conditions: Determination of hydric expansion coefficients by automated laser scanning. *Compos A Appl Sci Manuf* 2020;131:105803. <https://doi.org/10.1016/j.compositesa.2020.105803>.
- Gassan J, Bledzki AK. Thermal degradation of flax and jute fibers. *J Appl Poly Sci* 2001;82:1417–22.
- Siniscalco D, Arnould O, Bourmaud A, Le Duigou A, Baley C. Monitoring temperature effects on flax cell-wall mechanical properties within a composite material using AFM. *Polym Test* 2018;69:91–9. <https://doi.org/10.1016/j.polymertesting.2018.05.009>.
- Céline A, Fréour S, Jacquemin F, Casari P. The hygroscopic behavior of plant fibers: a review. *Front Chem* 2014;1:43. <https://doi.org/10.3389/fchem.2013.00043>.
- Mecklenburg MF. Determining the acceptable ranges of relative humidity and temperature in museums and galleries. Part 1, *Struct Response Relative Hum* 2007.
- Melelli A, Shah DU, Hapsari G, Cortopassi R, Durand S, Arnould O, et al. Lessons on textile history and fibre durability from a 4,000-year-old Egyptian flax yarn. *Nat Plants* 2021;7:1200–6. <https://doi.org/10.1038/s41477-021-00998-8>.
- Melelli A, Roselli G, Proietti N, Bourmaud A, Arnould O, Jamme F, et al. Chemical, morphological and mechanical study of the ageing of textile flax fibers from 17th/18th-century paintings on canvas. *J Cult Herit* 2021;52:202–14. <https://doi.org/10.1016/j.culher.2021.10.003>.
- Melelli A, Durand S, Arnould O, Richely E, Guessasma S, Jamme F, et al. Extensive investigation of the ultrastructure of kink-bands in flax fibres. *Ind Crop Prod* 2021; 164:113368. <https://doi.org/10.1016/j.indcrop.2021.113368>.
- Bos H. The Potential of Flax Fibres as Reinforcement for Composite Materials. 2004.
- Barbulée A, Jernot J-P, Bréard J, Gomina M. Damage to flax fibre slivers under monotonic uniaxial tensile loading. *Compos A Appl Sci Manuf* 2014;64:107–14. <https://doi.org/10.1016/j.compositesa.2014.04.024>.
- Wimmer R, Lucas B. Comparing mechanical properties of secondary wall and cell corner middle lamella in spruce wood. *IAWA J* 1997;18:77–88.
- Eder M, Arnould O, Dunlop JWC, Hornatowska J, Salmen L. Experimental micromechanical characterisation of wood cell walls. *Wood Sci Technol* 2013;47: 163–82.
- Jäger A, Bader Th, Hofstetter K, Eberhardsteiner J. The relation between indentation modulus, microfibril angle, and elastic properties of wood cell walls. *Compos A Appl Sci Manuf* 2011;42:677–85. <https://doi.org/10.1016/j.compositesa.2011.02.007>.
- Arnould O, Siniscalco D, Bourmaud A, Le Duigou A, Baley C. Better insight into the nano-mechanical properties of flax fibre cell walls. *Ind Crop Prod* 2017;97:224–8. <https://doi.org/10.1016/j.indcrop.2016.12.020>.
- Oliver WC, Pharr GM. An improved technique for determining hardness and elastic modulus using load and displacement sensing indentation experiments. *J Mat Res* 1992;7:1564–83.
- Derjaguin BV, Muller VM, Toporov YP. Effect of contact deformations on the adhesion of particles. *J Colloid Interface Sci* 1975;53:314–26.
- Melelli A, Durand S, Alvarado C, Kervoëlen A, Foucat L, Grégoire M, et al. Anticipating global warming effects: a comprehensive study of drought impact of both flax plants and fibres. *Ind Crops Prod* 2022;184. <https://doi.org/10.1016/j.indcrop.2022.115011>.
- Gindl W, Schoberl T. The significance of the elastic modulus of wood cell walls obtained from nanoindentation measurements. *Compos A Appl Sci Manuf* 2004;35: 1345–9.
- Guruprasad TS, Keryvin V, Charleux L, Guin J-P, Arnould O. On the determination of the elastic constants of carbon fibres by nanoindentation tests. *Carbon N Y* 2021; 173:572–86. <https://doi.org/10.1016/j.carbon.2020.09.052>.
- Adusumali R-B, Reifferscheid M, Weber H, Roeder T, Sixta H, Gindl W. Mechanical properties of regenerated cellulose fibres for composites. *Macromol Symp* 2006; 244:119–25. <https://doi.org/10.1002/masy.200651211>.
- Gindl W, Martinschitz KJ, Boesecke P, Keckes J. Structural changes during tensile testing of an all-cellulose composite by in situ synchrotron X-ray diffraction. *Compos Sci Technol* 2006;66:2639–47.
- Konnerth J, Gierlinger N, Keckes J, Gindl W. Actual versus apparent within cell wall variability of nanoindentation results from wood cell walls related to cellulose microfibril angle. *J Mater Sci* 2009;44:4399–406.
- Gorshkova T, Morvan C. Secondary cell-wall assembly in flax phloem fibres: role of galactans. *Planta* 2006;223:149–58.
- Yin Y, Berglund L, Salmén L. Effect of steam treatment on the properties of wood cell walls. *Biomacromolecules* 2011;12:194–202. <https://doi.org/10.1021/bm101144m>.
- Zickler GA, Schoberl T, Paris O. Mechanical properties of pyrolysed wood: a nanoindentation study. *Phil Mag* 2006;86:1373–86.
- Li Y, Yin L, Huang C, Meng Y, Fu F, Wang S, et al. Quasi-static and dynamic nanoindentation to determine the influence of thermal treatment on the mechanical properties of bamboo cell walls. *Holzforschung* 2015;69. <https://doi.org/10.1515/hf-2014-0112>.
- Xing D, Li J, Wang X, Wang S. In situ measurement of heat-treated wood cell wall at elevated temperature by nanoindentation. *Ind Crops Prod* 2016;87. <https://doi.org/10.1016/j.indcrop.2016.04.017>.
- Gindl W, Gupta H-S, Grünwald C. Lignification of spruce tracheid secondary cell walls related to longitudinal hardness and modulus of elasticity using nano-indentation. *Canadian J Bot* 2002;80:1029–33.
- Andreu-Lanoë GQAMC. Datations par le radiocarbone des tissus votifs du Gebel el-Zeit conservés au musée du Louvre. *Bulletin de l'Institut Français d'Archéologie Orientale Du Caire* 2011;111:23–34.
- Shaw I. Pharaonic quarrying and mining: settlement and procurement in Egypt's marginal regions. *Antiquity* 1994;68:108–19. <https://doi.org/10.1017/S0003598X0004624X>.
- Castel G. Gebel el-Zeit III. Les figurines féminines en terre cuite. *FIFAO* 2024;94.
- Ejsmond W, Skalec A, Chyla JM. The northern Necropolis of Gebel el-Zeit in light of old and current fieldwork. *J Egypt Archaeol* 2020;106:105–22. <https://doi.org/10.1177/0307513320970944>.
- Guillou E, Dumazert L, Caër C, Beigbeder A, Ouagne P, Le Saout G, et al. In-situ monitoring of changes in ultrastructure and mechanical properties of flax cell walls during controlled heat treatment. *Carbohydr Polym* 2023;321:121253. <https://doi.org/10.1016/j.carbpol.2023.121253>.
- Cohen SR, Kalfon-Cohen E. Dynamic nanoindentation by instrumented nanoindentation and force microscopy: a comparative review. *Beilstein J Nanotechnol* 2013;4:815–33. <https://doi.org/10.3762/bjnano.4.93>.
- Coq Germanicus R, Mercier D, Agrebi F, Fèbvre M, Mariolle D, Deschamps Ph, et al. Quantitative mapping of high modulus materials at the nanoscale: comparative study between atomic force microscopy and nanoindentation. *J Microsc* 2020;280: 51–62. <https://doi.org/10.1111/jmi.12935>.